

Fixed-Valve Micropump Simulation and Optimization—Designing for Specific Pressure-Flow Requirements

F.K. Forster* and T. Walter**

University of Washington

Department of Mechanical Engineering

Seattle, WA 98103-2600, USA

* forster@u.washington.edu

**tw80@u.washington.edu

ABSTRACT

Membrane pumps with fixed-geometry valves are extremely simple to fabricate and have the potential to be highly reliable and cheap due to their simplicity. We have recently implemented a means of optimizing design parameters based on calculated estimates of pressure rise and volume flow rate. While the method yields valuable information on which combination of parameters yields higher pressure or higher flow in a relative sense, calculated values are overly optimistic compared to measured values. In this study we investigated the role of entry and exit losses in the valves, which are not considered in the present model. The results show that including these effects is important, as they can raise valve resistance by a factor of five or more. Incorporation of these effects in the design process improved pump performance predictions and provides the capability of more accurately designing for higher pressure at the cost of less flow or vice versa, i.e. control of the pump performance curve.

Keywords: micropumps, fixed-valve, piezoelectric, low-order modeling, electronic cooling

1 INTRODUCTION

Micropumps have been one of the most reported topics in the area of small scale fluidic systems for well over a decade. However, choosing a pump technology to match a particular application is still very difficult due to the wide range of approaches including not only the ubiquitous reciprocating membrane and electroosmotic types but numerous others, such as electrohydrodynamic and magnetohydrodynamic types. In few cases are publications thorough enough to address the numerous constraints imposed by a particular fluidic application.

One class of reciprocating membrane pump that is the topic of this work is the fixed-valve piezoelectric membrane type. Fixed-valve means directional control of fluid flow is accomplished by shape alone with no moving parts. This idea has been around since at least the early part of the last century [4] and more recently [5]. Both are high Reynolds number macroscale devices and quite effective. The former example yields a differential flow ratio of 90 with gas as the working fluid. However,

since macro scale mechanical designs can be fabricated with outstanding performance, the fixed-geometry valve has virtually disappeared. The situation is different at the microscale and similar valves have been applied to micropumps as described in some of the earliest publications on the topic [6]–[8].

Our work addresses micropumps that utilize Tesla-type valves shown in Fig. 1. Their directional flow properties are based on differential flow paths in each direction as can be clearly seen in the figure. Another often used design is based on the diffuser, which derives its directional properties through flow separation in the direction of increasing cross-sectional area [9]. We use the Tesla-type valve primarily because it appears to be more easily modeled and has consistent performance as compared to the diffuser-type, since flow separation can be highly dependent on numerous factors. In either case, fixed-valve micropumps perform fairly well compared to mechanically-valved designs because, in part, they are tuned resonant devices that operate at relatively high frequency, which overcomes their lower valve efficiency and allows valve size to be tailored to optimize resonant behavior [10].

Previously, we have addressed four primary aspects of Tesla-type micropumps. In this report we address a fifth, which collectively completes a reasonable design approach. We demonstrate for the first time to our knowledge, control of a micropump’s pressure-flow characteristics through the proper choice of design parameters. This capability more readily allows the designer to tailor a pump to a particular application. Because of our current interests in liquid cooling of small electronic devices [11], [12] we have improved pressure rise capability and demonstrated a block-load pressure rise of approximately 2 psi [13]. Along with the stackable nature of these low profile pumps as demonstrated with four-pump stacked parallel networks [11], [12], we are closer to designs appropriate for electronic cooling applications.

The four principle areas mentioned above that led to the current study are optimization of piezoelectric driving elements [2], optimization of valve-shape [3], low-order linear modeling for efficient design of resonance [1], and a non-linear model for prediction of pressure rise and volume flow rate based on output from the lin-

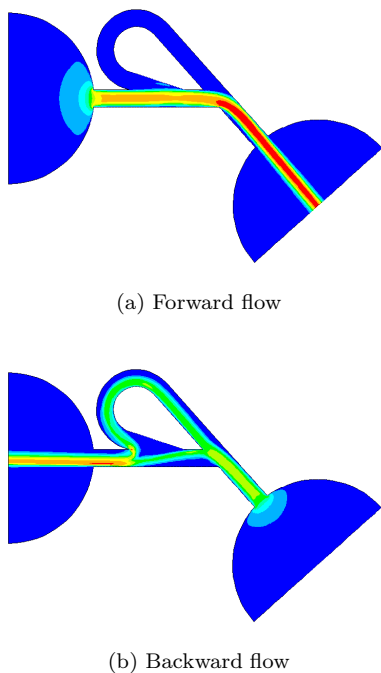


Figure 1: Optimally-shaped Tesla-type valve showing differential flow velocity patterns based on computational fluid dynamic simulation. Semi-circular regions model the pump chamber and plenums.

ear model [13]. In this report we address fluid dynamic entry and exit losses that can cause a significant departure from predictions based on fully developed flow, which was the basis for our model. This issue became apparent after the above-mentioned work failed to completely describe pump behavior. The effect of stiffness of the piezoelectric bimorph driver, fluid inertia and viscous resistance including entry and exit losses in the valves all require accurate handling for good modeling accuracy as they represent the fundamental aspects of even the simplest spring, mass and damper second-order dynamic system. The approach used to address the contribution of entry and exit losses to valve flow resistance are covered below followed by results and comparison to experiment.

2 METHODS

A low-order linear dynamic model [1], [13] treats each valve as a straight rectangular duct of length equal to the “straight through” centerline length L_f in the forward direction (see this flow path in Fig. 1(a)) and undergoing fully-developed oscillatory flow. The frequency dependent fluid inertance and resistance are determined from the exact solution of the Navier-Stokes equations [14]. The output harmonic amplitude of the volume flow rate for the highest voltage that can be applied to the

pump without cavitation or depoling of the PZT element is then used as a harmonic flow source to the two valves, which appear to the source as a pair of parallel branches, each containing resistance and inertance elements in series. The two resistance elements, which are oriented opposite to each other in the circuit, are modeled such that the reverse resistance R_r is equal to DiR_f , where R_f is the resistance calculated from the linear model and diodicity Di is the ratio of pressure drop in the reverse direction to that in the forward direction. Diodicity is calculated from computational fluid dynamics (CFD) modeling and is generally a function of Reynolds number, i.e. $Di(Re)$. No-load flow is calculated by solving non-linear differential equations for the DC level of flow through the simplified pump circuit described above. Block-load pressure is calculated as the DC level of pressure across a capacitor added to the outflow branch of the circuit. However, the amount of membrane motion calculated with the linear model is significantly greater than measured, and this results in significantly high overestimation of net flow and pressure [13].

The module developed to account for non-fully developed flow in the pump valves was based on well known quasi-steady formulas for entrance losses in laminar flow through rectangular ducts [15]. The magnitude of the effect was investigated by comparison of fully developed flow to that having entrance and exit losses. This was done in terms of the Darcy friction factor f_{darcy} which is related to pressure drop ΔP through a duct by the relation

$$\frac{\Delta P}{\frac{1}{2}\rho U^2} = f_{\text{darcy}} \left(\frac{L}{D_h} \right), \quad (1)$$

where ρ is mass density, U is the mean flow velocity, L is duct length and D_h is hydraulic diameter. For example, for a circular tube D_h is the actual tube diameter and $f_{\text{darcy}} = 64/Re$. Entry and exit effects are described by an effective friction factor f_{eff} and a loss factor K_{exit} such that Eq. (1) becomes

$$\frac{\Delta P}{\frac{1}{2}\rho U^2} = \left[f_{\text{eff}} + \frac{K_{\text{exit}}}{L/D_h} \right] \left(\frac{L}{D_h} \right). \quad (2)$$

The effect of these losses is shown in Fig. 2. Since the graph is presented in non-dimensional form, it applies to any size valve, laminar flow rate or fluid type. These results were used in modifications to the low-order linear model. Since pressure in Eqs. (1) and (2) can also be expressed as a product of volume flow rate and resistance $\Delta P = RQ$, an expression for resistance that includes the effects of non-fully developed flow can be expressed as

$$R_{\text{eff}} = \left[\frac{f_{\text{eff}} + K_{\text{exit}}/(L/D_h)}{f_{\text{darcy}}} \right] R. \quad (3)$$

An iterative process was used in the linear model to update this effective resistance until convergence using the

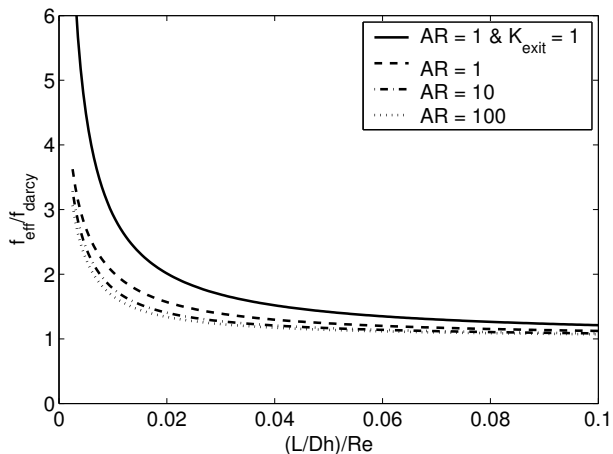


Figure 2: Ratio of the friction factor with entry losses to that for fully developed flow versus the ratio of normalized length to Reynolds number for a straight rectangular duct at various aspect ratios.

rms level of the valve Reynolds number as determined from the output of the linear system model. The converged value of the loss factor in brackets in Eq. (3) was then used to compute no-load flow and block-load pressure as described above.

The effect of non-fully developed flow on no-load flow and block-load pressure was then compared to experiment using a number of micropumps fabricated from plastic and having brass/PZT driving elements. Parts were modular so three thicknesses of brass and three valve sizes fabricated were used to assemble nine different pumps. The particular dimensions chosen corresponded to a region in a design space of membrane thickness and valve size where the combination of pressure and flow capability was considered to be a reasonable operating point in the design space [13].

3 RESULTS AND DISCUSSION

Modeling results and experiments were performed on pumps whose chamber diameter was 10 mm with chamber depth equal to valve depth. Membrane thickness of 76, 102 and 178 μm , and Tesla-type valves having channel widths of 150, 300 and 600 μm were used. The valve shape shown in Fig. 1, which is the optimal shape [3], had an aspect ratio (depth to width) of 2.5, and the path length in the forward direction L_f is 10.9 times valve width. For further details of the geometry see [3], [13]. All piezoelectric elements were PZT5A and 9 mm diameter. Figure 3 shows a typical assembled pump.

Table 1 shows measured and calculated values for block-load pressure P_{bl} and no-load flow rate Q_{nl} at a voltage excitation of 64 V 0-pk with the working fluid water at room temperature. Calculated values were generated with and without consideration of exit losses, i.e.

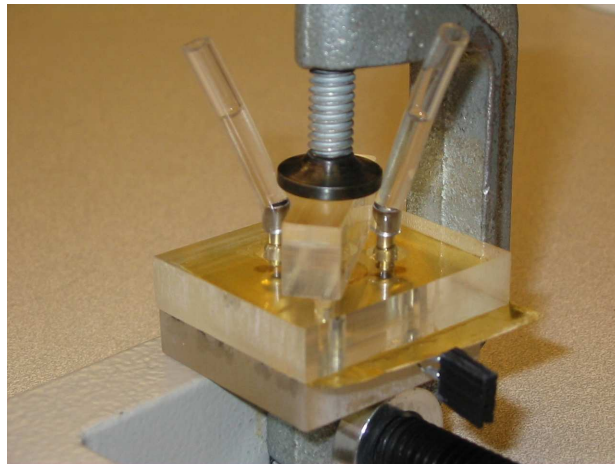


Figure 3: Assembled pump with interchangeable membrane/PZT driver (sandwiched between the two larger plastic blocks) and chamber/valves (bottom plastic block).

$K_{\text{exit}} = 1$ or 0. If outflow completely stops in the plenum chambers, i.e. $K_{\text{exit}} = 1$, the effect can be large as see from the two curves for an aspect ratio of unity at low values of $(L/D_h)/\text{Re}$ in Fig. 2). Since it is not clear whether stopped flow in the plenum is a valid assumption (see Fig. 1) this value represents an upper bound.

The calculated results agreed very well in terms of which pump generated the highest pressure, and reasonably well for which pump generated the highest flowrate. And although not shown in the table, pump P4 when driven at 125 V 0-pk generated approximately 2 psi [13]. However, the fully developed flow model seriously overestimated both pressure and flow. For the cases of entry loss only and entry plus exit loss, the calculated pressure is in much better agreement for pumps in columns 1 and 2 of Tab. 1. Pressure was underestimated for pumps in column 1 when the largest possible exit loss was considered suggesting that $K_{\text{exit}} = 1$ may be too large as discussed above. These results show that end losses can have a strong affect. They also suggest possible trade-offs between lowering Reynolds number with multiple parallel valves to move to the right in Fig. 2 if that does not yield significant decreases in directional flow capability of the valves, i.e. significantly decreased diodicity.

REFERENCES

- [1] Morris, C. J., and Forster, F. K., 2003. "Low-order modeling of resonance for fixed-valve micropumps based on first principles". *Journal of Microelectromechanical Systems*, **12**(3), pp. 325–334.
- [2] Morris, C. J., and Forster, F. K., 2000. "Optimization of a circular piezoelectric bimorph for a mi-

Table 1: Pump performance in terms of block-load pressure P_{bl} and no-load flow Q_{nl} for 64 V 0-pk excitation. FD = fully developed flow, I = inlet loss only and I/O = inlet and outlet loss. Pumps P1 through P9 are identified by the numbers in brackets corresponding to the design space coordinates [membrane thickness, valve width] in μm . Boxed values correspond to pumps with the highest pressure or flow, both measured and calculated.

loss type	P_{bl}		$Q_{N_{nl}}$		P_{bl}		$Q_{N_{nl}}$		P_{bl}		$Q_{N_{nl}}$	
	meas	calc	meas	calc	meas	calc	meas	calc	meas	calc	meas	calc
	kPa		ml/min		kPa		ml/min		kPa		ml/min	
	P1 [76,150]				P2 [76,300]				P3 [76,600]			
FD	2.3	11.25	1.1	9.37	0.89	6.29	1.7	19.65	0	1.93	0	22.99
I	2.3	3.57	1.1	3.22	0.89	3.42	1.7	11.95	0	1.91	0	22.85
I/O	2.3	1.52	1.1	1.49	0.89	1.67	1.7	6.14	0	1.68	0	20.56
	P4 [102,150]				P5 [102,300]				P6 [102,600]			
FD	4.5	13.3	1.4	10.45	1.3	5.45	1.8	16.36	0	1.70	0	19.04
I	4.5	4.09	1.4	3.48	1.3	3.93	1.8	12.78	0	1.69	0	18.95
I/O	4.5	1.76	1.4	1.62	1.3	2.32	1.8	7.81	0	1.67	0	18.71
	P7 [178,150]				P8 [178,300]				P9 [178,600]			
FD	4.3	12.73	1.4	7.59	0.55	3.89	0.78	10.2	0	1.17	0	11.17
I	4.3	5.32	1.4	3.85	0.55	3.82	0.78	10.0	0	1.16	0	11.14
I/O	4.3	2.66	1.4	2.06	0.55	3.04	0.78	8.46	0	1.16	0	11.08

- cropump driver”. *Journal of Micromechanics and Microengineering*, **10**(3), pp. 459–465.
- [3] Gamboa, A. R., Morris, C. J., and Forster, F. K., 2005. “Improvements in fixed-valve micropump performance through shape optimization of valves”. *Journal of Fluids Engineering*, **FED-127**(March), pp. 339–346.
- [4] Tesla, N., 1920. Valvular conduit. U.S. Patent No. 1,329,559.
- [5] Reed, J. L., 1993. Fluidic rectifier. U. S. Patent No. 5,265,636, Nov. 30.
- [6] Olsson, A., Enoksson, P., Stemme, G., and Stemme, E., 1995. “A valve-less planar pump in silicon”. In *Transducers '95 (Stockholm)*, Vol. 2, IEEE, pp. 291–294.
- [7] Forster, F., Bardell, R., Afromowitz, M., and Sharma, N., 1995. “Design, fabrication and testing of fixed-valve micropumps”. In *Proceedings of the ASME Fluids Engineering Division 1995 (San Francisco)*, D. C. Wiggert et al., eds., Vol. FED-234, ASME, pp. 39–44.
- [8] Gerlach, T., Schuenemann, M., and Wurmus, H., 1995. “A new micropump principle of the reciprocating type using pyramidal micro flowchannels as passive valves”. *Journal of Micromechanics and Microengineering*, **5**, pp. 199–201.
- [9] Gamboa, A. R., and Forster, F. K., 2004. “Is there a best fixed-geometry valve for micropumps?”. In *Proceedings of the ASME Fluids Engineering Division 2004 (Anaheim)*.
- [10] Gamboa, A. R., 2004. “Shape optimization of the nozzle-diffuser and tesla-type valves for applications in micropumps”. M. S. Thesis, University of Washington, Seattle.
- [11] Morris, C. J., Chung, J. Y., Rahm, P. E., Forster, F. K., Shekarriz, R., and Faulkner, D., 2004. “Electronic cooling systems based on fixed-valve micropump networks”. In *Solid-State Sensor, Actuator and Microsystems Workshop, Transducers Research Foundation, Inc.*, pp. 152–155.
- [12] Faulkner, D., Ward, C., Gilbuena, D., Shekarriz, R., and Forster, F. K., 2006. “Fixed valve piezoelectric micropump for miniature thermal management module”. In *Proceedings of the ASME Fluids Engineering Division Summer Meeting and Exhibition (Miami)*.
- [13] Forster, F. K., and Walter, T., 2007 (in press). “Design optimization of fixed-valve micropumps for miniature cooling system”. In *Proceedings of the ASME/JSME Thermal Engineering and Summer Heat Transfer Conferences & InterPACK 07 (Vancouver B.C. July 8–12)*.
- [14] Morris, C. J., and Forster, F. K., 2004. “Oscillatory flow in microchannels: comparison of exact and approximate impedance models with experiment”. *Experiments in Fluids*, **36**(6), pp. 928–937.
- [15] White, F. M., 1991. *Viscous Fluid Flow*, 2nd ed. McGraw-Hill, Inc., New York.

Fixed-Valve Micropump Simulation and Optimization—Designing for Specific Pressure-Flow Requirements

F.K. Forster*¹ and T. Walter**

University of Washington

Department of Mechanical Engineering

Seattle, WA 98103-2600, USA

* forster@u.washington.edu

**tw80@u.washington.edu

ABSTRACT

Membrane pumps with fixed-geometry valves are extremely simple to fabricate and have the potential to be highly reliable and cheap due to their simplicity. We have recently implemented a means of optimizing design parameters based on calculated estimates of pressure rise and volume flow rate. While the method yields valuable information on which combination of parameters yields higher pressure or higher flow in a relative sense, actual calculated values are overly optimistic compared to measured values. In this study we investigated the role of entry and exit losses in the valves, which are not considered in the present model. The results show that including these effects is important, as they can raise valve resistance by a factor of five or more. Incorporation of these effects in the design process improved pump performance predictions and provides the capability of more accurately designing for higher pressure at the cost of less flow or vice versa, i.e. control of the pump performance curve.

Keywords: micropumps, fixed-valve, piezoelectric, low-order modeling, electronic cooling

1 INTRODUCTION

Micropumps have been one of the most reported topics in the area of small scale systems for well over a decade. However, choosing a pump technology to match a particular application is still very difficult due to wide range of approaches including not only the ubiquitous reciprocating membrane and electroosmotic types but numerous others, such as electrohydrodynamic and magnetohydrodynamic types. In few cases are publications thorough enough to address the numerous constraints imposed by a particular fluidic application.

One class of reciprocating membrane pump that is the topic of this work is the fixed-valve piezoelectric membrane type. Fixed-valve means directional control of fluid flow is accomplished by shape alone with no moving parts. This idea has been around since at least the early part of the last century [4] and more recently [5]. Both are high Reynolds number macroscale devices and quite effective. The former example yields a differential flow ratio of 90 with gas as the working fluid. However,

since macro scale mechanical designs can be fabricated with outstanding performance, the fixed-geometry valve has virtually disappeared. The situation is different at the microscale and similar valves have been applied to micropumps as described in some of the earliest publications on the topic [6]–[8].

Our work addresses micropumps that utilize tesla-type valves shown in Fig. 1. Their directional flow properties are based on differential flow paths in each direction as can be clearly seen in the figure. Another often used design is based on the diffuser, which derives its directional properties through flow separation in the direction of increasing cross-sectional area [9]. We use the tesla-type valve primarily because it appears to be more easily modeled and has consistent performance as compared to the diffuser-type, since flow separation can be highly dependent on numerous factors. In either case, fixed-valve micropumps perform fairly to mechanically-valved designs because they are tuned resonant devices that operate at relatively high frequency, which overcomes lower valve efficiency and allows valve size to be tailored to optimize resonant behavior [10].

Previously, we have addressed four primary aspects of tesla-type micropumps. In this report we address a fifth, which collectively completes a reasonable design approach. We demonstrate for the first time to our knowledge, control of a micropump’s pressure-flow characteristics through the proper choice of design parameters. This capability more readily allows the designer to tailor a pump to a particular application. Because of our current interests in liquid cooling of small electronic devices [11], [12] we have improved pressure rise capability and demonstrated a block load pressure rise of approximately 2 psi [13]. Along with the stackable nature of these low profile pumps as demonstrated with four-pump stacked parallel networks [11], [12], we are closer to designs appropriate for electronic cooling applications.

The four principle areas mentioned above that led to the current study are optimization of piezoelectric driving elements [2] optimization of valve-shape [3], low-order linear modeling for efficient design of resonance [1], and a non-linear module for prediction of pressure rise and volume flow rate based on output from the linear

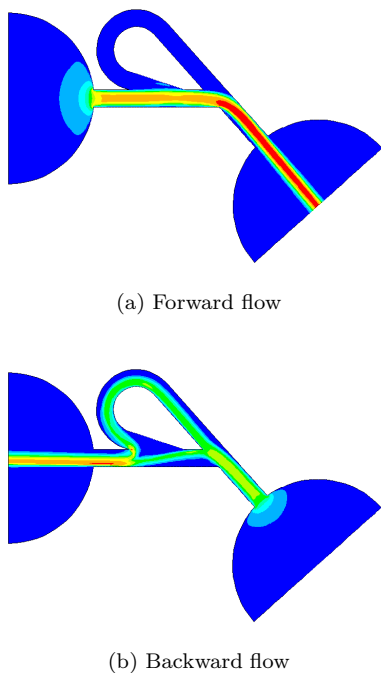


Figure 1: Optimally-shaped tesla-type valve showing differential flow patterns based on computational fluid dynamic simulation.

model [13]. In this report we address fluid dynamic entry and exit losses that can cause a significant departure from predictions based on fully developed flow, which was the basis of our model. This issue became apparent after the above-mentioned work failed to completely describe pump behavior. The effect of stiffness of the piezoelectric bimorph driver, fluid inertia and viscous resistance including entry and exit losses in the valves all require accurate handling for good modeling accuracy as they represent the fundamental aspects of even the simplest spring, mass and damper second-order dynamic system. The approach used to address the contribution of entry and exit losses to valve flow resistance are covered below followed by results and comparison to experiment.

2 METHODS

A low-order linear dynamic model [1], [13] treats each valve as a straight rectangular duct of length equal to the “straight through” length L_f in the forward direction (see Fig. 1) and undergoing fully-developed oscillatory flow. The frequency dependent fluid inertance and resistance are determined from the exact solution of the Navier-Stokes equations [14]. The output harmonic amplitude the volume flow rate for the highest voltage that can be applied to the pump without cavitation or depoling of the PZT element is then used as a harmonic flow

source to the two valves, which appear to the source as a pair of parallel branches, each containing resistance and inertance elements in series. The two resistance elements, which are oriented opposite to each other in the circuit, are modeled such that the reverse resistance R_r is equal to DiR_f , where R_f is the resistance calculated from the linear model and diodicity Di is the ratio of pressure drop in the reverse direction to that in the forward direction. Diodicity is calculated from computational fluid dynamics (CFD) modeling and is generally a function of Reynolds number, i.e. $Di(Re)$. No-load flow is calculated by solving non-linear differential equations for the DC level of flow through the simplified pump circuit described above. Block load pressure is calculated as the DC level of pressure across a capacitor added to the outflow branch of the circuit. However, the amount of membrane motion calculated with the linear model is significantly greater than measured and, this results in significantly high over estimation of net flow and pressure [13].

The module developed to account for non-fully developed flow in the pump valves was based on well known quasi-steady formulas for entrance losses in laminar flow through rectangular ducts [15]. The magnitude of the effect was investigated by comparison of fully developed flow to that having entrance and exit losses. This was done in terms of the Darcy friction factor f_{darcy} which is related to pressure drop ΔP through a duct by the relation

$$\frac{\Delta P}{\frac{1}{2}\rho U^2} = f_{\text{darcy}} \left(\frac{L}{D_h} \right), \quad (1)$$

where ρ is mass density, U is the mean flow velocity, L is duct length and D_h is hydraulic diameter. For example, for a circular tube D_h is the actual tube diameter and $f_{\text{darcy}} = 64/Re$. Entry and exit effects are described by an effective friction factor f_{eff} and a loss factor K_{exit} such that Eq. (1) becomes

$$\frac{\Delta P}{\frac{1}{2}\rho U^2} = \left[f_{\text{eff}} + \frac{K_{\text{exit}}}{L/D_h} \right] \left(\frac{L}{D_h} \right). \quad (2)$$

The effect of these losses is shown in Fig. 2. Since the graph is presented in non-dimensional form, it applies to any size valve, laminar flow rate or fluid type. These results were used in modifications to the low-order linear model. Since pressure in Eqs. (1) and (2) can also be expressed as a product of volume flow rate and resistance $\Delta P = RQ$, an expression for resistance that includes the effects of non-fully developed flow can be expressed as

$$R_{\text{eff}} = \left[\frac{f_{\text{eff}} + K_{\text{exit}}/(L/D_h)}{f_{\text{darcy}}} \right] R. \quad (3)$$

An iterative process was used in the linear model to update this effective resistance until convergence using the

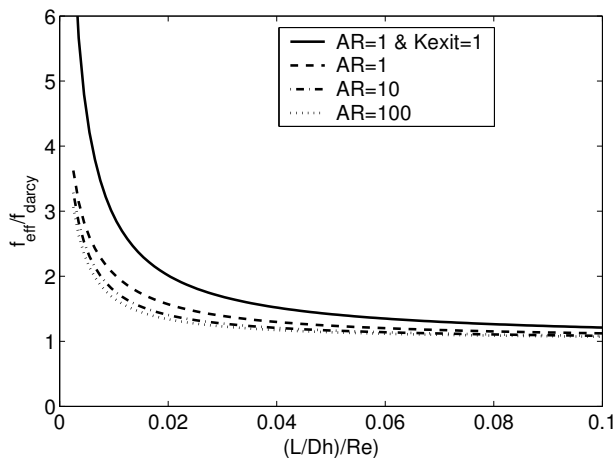


Figure 2: Ratio of the friction factor with end losses to that for fully developed flow versus the ratio of normalized length to Reynolds number for a straight rectangular duct at various aspect ratios.

rms level of the valve Reynolds number as determined from the output of the linear system model. The converged value of the loss factor in brackets in Eq. (3) number was then used to compute no-load flow and block-load pressure as described above.

The effect of non-fully developed flow on no-load flow and block-load pressure was then compared to experiment using a number of micropumps fabricated from plastic and having brass/PZT driving elements. Parts were modular so three thicknesses of brass and three valve sizes fabricated were used to assemble nine different pumps. The particular dimensions chosen correspond to a region in a design space of membrane thickness and valve size where the combination of pressure and flow capability were best according to calculations [13].

3 RESULTS AND DISCUSSION

Modeling results and experiments were performed on pumps whose chamber diameter was 10 mm with chamber depth equal to valve depth. Membrane thickness of 76, 102 and 178 μm , and tesla-type valves having channel widths of 150, 300 and 600 μm were used. The valve shape shown in Fig. 1, which is the optimal shape [3], had an aspect ratio (depth to width) of 2.5, and the path length in the forward direction L_f is 10.9 times valve width. For further details of the geometry see [3], [13]. All piezoelectric elements were PZT5A and 9 mm diameter. Figure 3 shows a typical assembled pump.

Table 1 shows measured and calculated values for block-load pressure P_{bl} and no-load flow rate Q_{nl} at a voltage excitation of 64 V with the working fluid water at room temperature. Calculated values were generated with and without consideration of exit losses, i.e. K_{exit}

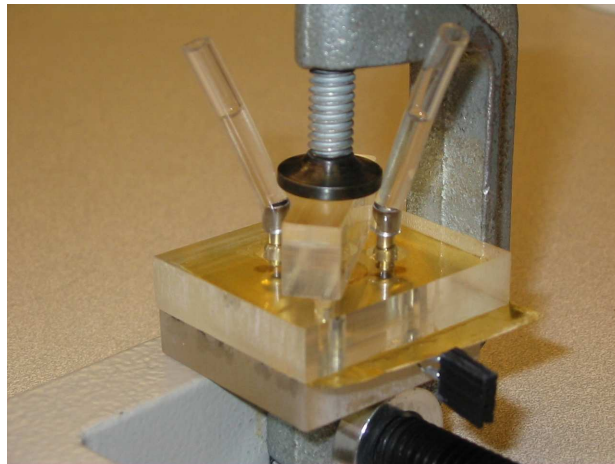


Figure 3: Captions capitalized in sentence case without a period.

= 1 or 0. If outflow completely stops in the plenum chambers, $K_{\text{exit}} = 1$, the effect of which (the difference between the two curves for aspect ratio of unity in Fig. 2) is quite large. Since it is not clear whether stopped flow in the plenum is a valid assumption (see Fig. 1) this value represents an upper bound.

The calculated results agreed very well in terms of which pump generated the highest pressure and reasonably well for flow. And although not shown in the table, pump P4 when driven at 125 volts generated approximately 2 psi[13]. However, the fully developed flow model seriously over estimated both pressure and flow. For the cases of entry loss only and entry plus exit loss, the calculated pressure is in much better agreement for pumps in columns 1 and 2 of Tab. 1. Pressure was underestimated for pumps in column 1 when the largest possible exit loss was considered suggesting that $K_{\text{exit}} = 1$ may be too large as discussed above. These results show that end losses can have a strong affect. It also suggests possible trade-offs between lowering Reynolds number with multiple parallel valves to move to the right in Fig. 2 if that does not lead to significant decrease in directional flow capability of the valves, i.e. lower diodicity.

REFERENCES

- [1] Morris, C. J., and Forster, F. K., 2003. "Low-order modeling of resonance for fixed-valve micropumps based on first principles". *Journal of Microelectromechanical Systems*, **12**(3), pp. 325–334.
- [2] Morris, C. J., and Forster, F. K., 2000. "Optimization of a circular piezoelectric bimorph for a micropump driver". *Journal of Micromechanics and Microengineering*, **10**(3), pp. 459–465.
- [3] Gamboa, A. R., Morris, C. J., and Forster, F. K., 2005. "Improvements in fixed-valve micropump

Table 1: pump performance in terms of block-load pressure P_{bl} and no-load flow Q_{nl} for 64 V 0-peak excitation. FD = fully developed flow, I = inlet loss only and I/O = inlet and outlet loss. Pumps P1 through P9 are identified by the numbers in brackets corresponding to the design space coordinates [membrane thickness, valve width] in μm . Boxed values correspond to pumps with the highest pressure or flow, both measured and calculated.

loss type	P_{bl}		$Q_{N_{nl}}$		P_{bl}		$Q_{N_{nl}}$		P_{bl}		$Q_{N_{nl}}$	
	meas	calc	meas	calc	meas	calc	meas	calc	meas	calc	meas	calc
	kPa		ml/min		kPa		ml/min		kPa		ml/min	
	P1 [76,150]				P2 [76,300]				P3 [76,600]			
FD	2.3	11.25	1.1	9.37	0.89	6.29	1.7	19.65	0	1.93	0	22.99
I	2.3	3.57	1.1	3.22	0.89	3.42	1.7	11.95	0	1.91	0	22.85
I/O	2.3	1.52	1.1	1.49	0.89	1.67	1.7	6.14	0	1.68	0	20.56
	P4 [102,150]				P5 [102,300]				P6 [102,600]			
FD	4.5	13.3	1.4	10.45	1.3	5.45	1.8	16.36	0	1.70	0	19.04
I	4.5	4.09	1.4	3.48	1.3	3.93	1.8	12.78	0	1.69	0	18.95
I/O	4.5	1.76	1.4	1.62	1.3	2.32	1.8	7.81	0	1.67	0	18.71
	P7 [178,150]				P8 [178,300]				P9 [178,600]			
FD	4.3	12.73	1.4	7.59	0.55	3.89	0.78	10.2	0	1.17	0	11.17
I	4.3	5.32	1.4	3.85	0.55	3.82	0.78	10.0	0	1.16	0	11.14
I/O	4.3	2.66	1.4	2.06	0.55	3.04	0.78	8.46	0	1.16	0	11.08

- performance through shape optimization of valves”. *Journal of Fluids Engineering*, **FED-127**(March), pp. 339–346.
- [4] Tesla, N., 1920. Valvular conduit. U.S. Patent No. 1,329,559.
- [5] Reed, J. L., 1993. Fluidic rectifier. U. S. Patent No. 5,265,636, Nov. 30.
- [6] Olsson, A., Enoksson, P., Stemme, G., and Stemme, E., 1995. “A valve-less planar pump in silicon”. In *Transducers '95 (Stockholm)*, Vol. 2, IEEE, pp. 291–294.
- [7] Forster, F., Bardell, R., Afromowitz, M., and Sharma, N., 1995. “Design, fabrication and testing of fixed-valve micropumps”. In *Proceedings of the ASME Fluids Engineering Division 1995 (San Francisco)*, D. C. Wiggert et al., eds., Vol. FED-234, ASME, pp. 39–44.
- [8] Gerlach, T., Schuenemann, M., and Wurmus, H., 1995. “A new micropump principle of the reciprocating type using pyramidic micro flowchannels as passive valves”. *Journal of Micromechanics and Microengineering*, **5**, pp. 199–201.
- [9] Gamboa, A. R., and Forster, F. K., 2004. “Is there a best fixed-geometry valve for micropumps?”. In *Proceedings of the ASME Fluids Engineering Division 2004 (Anaheim)*.
- [10] Gamboa, A. R., 2004. “Shape optimization of the nozzle-diffuser and tesla-type valves for applications in micropumps”. M. S. Thesis, University of Washington, Seattle.
- [11] Morris, C. J., Chung, J. Y., Rahm, P. E., Forster, F. K., Shekarriz, R., and Faulkner, D., 2004. “Electronic cooling systems based on fixed-valve micropump networks”. In *Solid-State Sensor, Actuator and Microsystems Workshop, Transducers Research Foundation, Inc.*, pp. 152–155.
- [12] Faulkner, D., Ward, C., Gilbuena, D., Shekarriz, R., and Forster, F. K., 2006. “Fixed valve piezoelectric micropump for miniature thermal management module”. In *Proceedings of the ASME Fluids Engineering Division Summer Meeting and Exhibition (Miami)*.
- [13] Forster, F. K., and Walter, T., 2007 (in press). “Design optimization of fixed-valve micropumps for miniature cooling system”. In *Proceedings of the ASME/JSME Thermal Engineering and Summer Heat Transfer Conferences & InterPACK 07 (Vancouver B.C. July 8–12)*.
- [14] Morris, C. J., and Forster, F. K., 2004. “Oscillatory flow in microchannels: comparison of exact and approximate impedance models with experiment”. *Experiments in Fluids*, **36**(6), pp. 928–937.
- [15] White, F. M., 1991. *Viscous Fluid Flow*, 2nd ed. McGraw-Hill, Inc., New York.